ELSEVIER

Polymer 41 (2000) 1011–1025

polymer

Miscible PS/PPE compounds: an alternative for blend phase morphology studies? Influence of the PPE content on the surface tension of PS/PPE and on the interfacial tension in PP/(PS/PPE) and POM/(PS/PPE) blends

V. Everaert[a], G. Groeninckx[a,*], J. Pionteck[b], B.D. Favis[c], L. Aerts[d], P. Moldenaers[e], J. Mewis[e]

[a]Laboratory for Macromolecular Structural Chemistry, Department of Chemistry, Catholic University of Leuven, Celestijnenlaan 200F, B-3001 Heverlee, Belgium
[b]Institute for Polymer Research Dresden, Hohe Strasse 6, D-01069, Dresden, Germany
[c]Department of Chemical Engineering, Ecole Polytechnique de Montréal, P.O. Box 6079, Station Centre Ville, Montréal, Québec, Canada H3C 3A7
[d]Dow Benelux N.V., P.O. Box 48, 4530 Terneuzen, The Netherlands
[e]Catholic University of Leuven, de Croylaan 46, B-3001 Heverlee, Belgium

Received 1 January 1999; accepted 15 March 1999

Abstract

The influence of the PPE content in a miscible PS/PPE phase on the surface tension and polarity of PS/PPE mixtures, and on the interfacial tension in PP/(PS/PPE) and POM/(PS/PPE) blend systems was investigated. Surface tensions, $\sigma(T)$, and polarity, x_p, were experimentally determined by means of the pendant drop analysis technique, and were compared to the values predicted theoretically via Macleod's theory. The interfacial tension, σ_{12}, was determined both from the dynamic breaking thread method, and from the pendant drop analysis, which is an equilibrium method. The experimental values were compared to those predicted from the harmonic mean equation. Good agreement was found between the absolute values for σ_{12} obtained from both the techniques. The *surface tension* of the PS/PPE mixtures, in a temperature range of 230–260°C, appears to be unaffected by the presence of PPE, within the experimental error of the measurements. These findings were in good agreement with the prediction of $\sigma(T)$ from Macleod's theory. The *interfacial tension* of the PP/(PS/PPE) or POM/(PS/PPE) blend systems did not seem to be affected significantly when using a PS/PPE phase with a higher content of PPE. Finally, calculations showed that PPE causes the polarity of the PS/PPE mixtures to increase slightly from a value of 0.17 for pure PS to 0.20 for pure PPE. © 1999 Published by Elsevier Science Ltd. All rights reserved.

Keywords: PS/PPE mixtures; PP/(PS/PPE) blends; POM/(PS/PPE) blends

1. Introduction

The properties of immiscible polymer blends depend to a large extent on the flow-induced morphology formed during melt-blending and further processing. As the industrial importance of such systems still increases, it becomes extremely important to understand the complex matter of all factors controlling the phase morphology development. Development of the phase morphology during melt-mixing of immiscible polymeric materials has been studied in many papers, most of them focussing on the influence of processing conditions, blend composition and melt-viscosity ratio. Only limited attention has been paid to the influence of the interfacial tension, which also has been shown to have a significant impact on the blend properties [1–5]. One of the main reasons for this neglect is that only few reliable methods exist for measuring surface and/or interfacial tensions in viscoelastic polymer melts.

Up to now, the majority of studies devoted to the influence of the melt-viscosity ratio of the components in immiscible blend systems on the phase morphology development, have been performed by varying the molecular weight (MW) of the components, assuming that the interfacial tension remains unaffected [6–10]. The latter assumption is mainly based on the work of Anastasiadis et al. [11], who investigated the interfacial tension between polystyrene (PS) and polymethylmethacrylate (PMMA), as a function of the MW of PS. These authors found that an increase of the MW leads to an increase of the interfacial tension, but when the MW becomes larger than the critical MW for entanglements, this increase becomes negligible. This was related to the entropic adsorption of chain ends to the interfacial region [12]. However, other authors reported that the interfacial tension between two polymers increases

---

* Corresponding author.

0032-3861/00/$ - see front matter © 1999 Published by Elsevier Science Ltd. All rights reserved.
PII: S0032-3861(99)00239-6

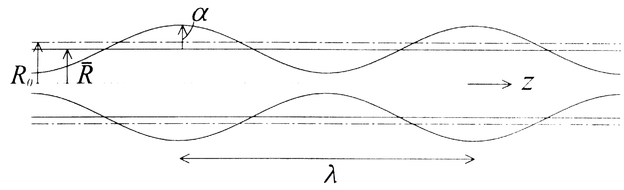

Fig. 1. Sinusoidal distortion imposed on a liquid thread embedded in a melt matrix, as a consequence of capillary instabilities.

with increasing MW [13–15] and decreases with increasing polydispersity [13]. As a consequence, care should be taken when evaluating the influence of the melt-viscosity ratio on the phase morphology in immiscible blend systems by varying the MW of the components.

In this research project, an alternative model system has been selected to study the influence of the melt-viscosity ratio in an immiscible polymer blend on its blend phase morphology [16,17]. A broad range of melt-viscosity ratios could be obtained by making use of the miscible polystyrene/poly(2,6-dimethyl-1,4-phenylene ether) (PS/PPE) system. Blends of PS ($T_g = 102$°C) with PPE ($T_g = 215$°C) are miscible over the whole composition range [18,19]. As such, any desired melt-viscosity can be obtained by simply varying the PS/PPE blend composition.

PPE is an amorphous engineering thermoplastic on which up to now not much research has been published with respect to surface and/or interfacial tension. However, there exist indications that the surface tension of PS and PPE would be comparable [20]. If this be the case, the surface tension of any of the miscible PS/PPE blends would be constant over the whole composition range. Consequently, miscible PS/PPE blends offer a valuable alternative for studies in which it is required to vary the melt-viscosity ratio without affecting the interfacial tension in the system.

For this paper, both the dynamic breaking thread method and the equilibrium pendant drop analysis method were used to evaluate the influence of the PPE content in the PS/PPE phase on the surface and/or interfacial tension in polypropylene/(PS/PPE) and poly(oxymethylene)/(PS/PPE) systems.

2. The breaking thread method

2.1. Theory

The capillary break-up method to experimentally determine the interfacial tension, σ_{12}, between two polymeric materials is based on the theory of Tomotika [21,22]. The author generalized the phenomenon of break-up by capillary instabilities as described by Rayleigh [23] for waterjets in air, to viscous Newtonian threads embedded in a viscous Newtonian matrix.

The growth of these capillary instabilities is described as a sinusoidal distortion with amplitude α imposed on the interface of a liquid cylinder (Fig. 1):

$$R(z) = \bar{R} + \alpha \sin\left(\frac{2\pi z}{\lambda}\right), \quad (1)$$

where $\bar{R} = (R_0^2 - \alpha^2/2)^{1/2}$ is the average thread radius (in m), R_0 the initial thread radius (in m), α the amplitude of the distortion (in m), λ the wavelength of the distortion (in m) and z the coordinate along the thread (in m).

Only distortions having a wavelength, λ, larger than the

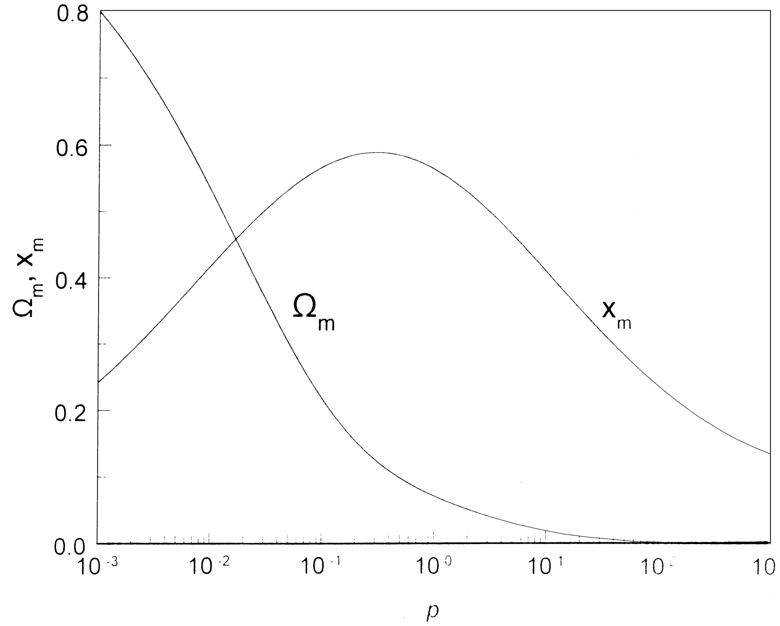

Fig. 2. Dominant wave number, X_{max}, and the corresponding dimensionless growth rate, Ω_{max}, as a function of the viscosity ratio, p.

Table 1
Material characteristcs

Material	MFI (g/10 min)	M_n (GPC) (g/mol)	M_w (GPC) (g/mol)	Polydispersity	Density (g/cm^3)
PP12	12(230°C)	46 400[a]	260 000[a]	5.6	0.89
PP40	40(230°C)	50 200[a]	215 000[a]	4.3	0.91
PS	–	81 900[b]	190 000[b]	2.6	1.055
PPE	13(300°C)	19 300[b]	54 300[b]	2.8	1.065
POM	–	–	± 70 000	–	± 1.4

[a] Measured in TCB at 140°C; molecular weights are based on polyethylene standards and multiplied with a factor 1.55 (calculated from the Mark–Houwink constants for PP and PE) (Scholte, Meijerink, Schoffeleers and Brands, J Appl Polym Sci 29 (1984)).

[b] Measured in THF at 25°C; molecular weights are based on polystyrene standards.

circumference of the thread ($\lambda > 2\pi R_0$) can grow further, because they cause an effective decrease of the total interfacial area. The growth of the distortions proceed exponentially with time, t:

$$\alpha = \alpha_0 \exp(qt), \tag{2}$$

where α_0 is the distortion amplitude at $t = 0$ (in m), and q is the growth rate of the distortions (in s^{-1}) as described by

$$q = \frac{\sigma_{12}}{2\eta_m R_0}\Omega(X,p), \tag{3}$$

where σ_{12} is the interfacial tension (N/m), η_m the zero shear viscosity of the matrix (Pa s), $p = \eta_d/\eta_m$ the viscosity ratio at zero shear conditions, η_d the zero shear viscosity of the thread (Pa s), $X = (2\pi R_0)/\lambda$ the experimentally observed wavenumber, and $\Omega(X,p)$ the dimensionless growth rate function.

The function $\Omega(X,p)$ has been tabulated by Tomotika [21,22] for break-up at the dominant wavelength, $\lambda_{\max}$, where the growth rate of the distortion becomes the fastest, and hence is expected to lead to the final thread break-up. Fig. 2 shows the dominant wavenumber, $X_m = (2\pi R_0)/\lambda_{\max}$, and the corresponding growth rate function, $\Omega(X_m,p)$, as a function of the viscosity ratio, p.

A more complete description of the growth rate function, $\Omega(X,p)$, for thread break-up at non-dominant wavenumbers has been given by Chappelear [24] and Palierne and Lequeux [25]. The corresponding curves have been computed for a viscosity ratio range of 0.001–1000 by Luciani et al. [26]. A complete three-dimensional plot of $\Omega(X,p)$ as a function of both p and X is presented in the work of Machiels et al. [27].

Thread break-up is completed when the amplitude of the distortions, α, equals the average radius, $R = 0.81R_0$ [28]. Hence, the time required for thread break-up, t_b, can be estimated from

$$t_b = \frac{1}{q}\ln\left(\frac{0.81R_0}{\alpha_0}\right). \tag{4}$$

Kuhn [29] derived an expression for the initial distortion of the interface, α_0, based on thermal fluctuations of the interface (Brownian motions):

$$\alpha_0 = \left(\frac{21kT}{8\pi^{3/2}\sigma_{12}}\right)^{1/2}, \tag{5}$$

where k is the Boltzmann constant (1.3807×10^{-23} J/K), and T is the absolute temperature (in K).

Substitution of the distortion growth rate, q (Eq. (3)), and α_0 (Eq. (5)) in Eq. (4) yields an expression to estimate the time scale of the experiments:

$$t_b = \frac{\eta_m R_0}{\Omega(X_m,p)\sigma_{12}}\ln\left(\frac{10^{23}\sigma_{12}R_0^2}{T}\right). \tag{6}$$

2.2. Advantages and limitations of the breaking thread method

The breaking thread method is a dynamic method suited to estimate interfacial tensions in a wide range of polymeric systems. The method is relatively simple and requires no use of highly specialized equipment. The most limiting factor is the requirement of accurate zero shear viscosity data at each measurement temperature. The relatively short break-up times, usually less than 10 min, allows us to minimize the degradation problems, which could drastically affect the value of σ_{12}; low molecular weight degradation products are known to migrate preferentially to the polymer interface, thereby lowering the measured interfacial tension [30]. Further, the method is also suitable for systems consisting of polymers with small density differences and for systems with relatively high viscosities, where alternative methods such as the pendant or spinning drop method require several hours to attain an equilibrium shape. Although it was advised not to exceed a thread viscosity of 10^5 Pa s; systems with a viscosity ratio $\eta_d/\eta_m \ll 1$ are expected to give the best results [31]. However, it still remains an absolute precondition that the polymer shows Newtonian behavior as the shear rate approximates zero [31], in order to be able to apply the theory developed by Tomotika [21,22].

2.3. Experimental

2.3.1. Materials

An overview of the material characteristics is given in

Table 2
Characteristics of the miscible amorphous PS/PPE phases

Blend composition	Code name	T_g (DSC) (°C)	T_g range (°C)
PS/PPE 100/0	Ha1[a]	102	96–106
PS/PPE 90/10	Ha3	109	105–114
PS/PPE 75/25	Ha5	122.5	114–129
PS/PPE 50/50	Ha7	144	134–155

[a] In order to estimate the degree of degradation caused by this mixing operation, the molecular weight of Ha1 was determined both from GPC and viscosimetry. A value for M_n of 70 000 and M_w of 170 000 was found, which implies a decrease of the molecular weight of PS by 10%.

Table 1. The polypropylene (PP) used in this study was a commercial grade isotactic PP12 supplied by Atochem. Its melting point is 161°C. From the same supplier, a low molecular weight PP40 was obtained. The PS was a commercial grade Styron® E680 supplied by Dow Benelux N.V. (The Netherlands). The poly(2,6-dimethyl-1,4-phenylene ether) (PPE) was a PPE-800 grade supplied by the General Electric (The Netherlands). The polymethylene oxide (POM) was a commercial grade POM-copolymer, Celcon® M-50 from Hoechst Celanese (USA), containing ±5 wt.% ethyleneglycol to stabilize the product against depolymerization at elevated temperatures. Its melting point is 175°C.

2.3.2. Preparation of the amorphous PS/PPE phases

The amorphous phases were prepared by melt-blending PS ($T_g = 102$°C) with PPE ($T_g = 215$°C); both the components are perfectly miscible over the whole composition range [18,19]. Blending was performed on a Haake Rheocord 90 twin screw extruder after drying the materials overnight at 40°C under vacuum. The mixing conditions were set as follows: screw speed, 120 rpm; intake section, 200°C; melting section, 300°C; section 3 to 5, 285°C; throughput, 10–15 g/min. At the die exit, strands were cooled in a water bath and pelletized. The homogeneity of each blend was checked by DSC measurements. Table 2 presents a list of the prepared amorphous phases and the corresponding T_g's.

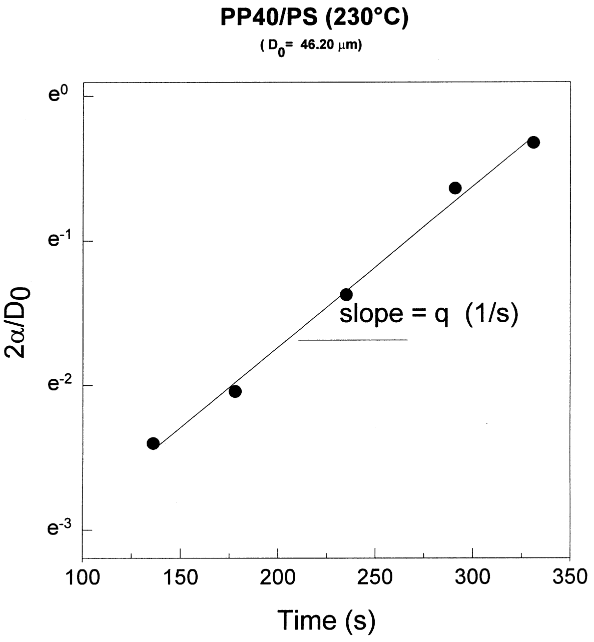

Fig. 3. Experimental determination of the exponential growth rate of capillary instabilities, q, as a function of time from thread break-up experiments.

2.3.3. Rheological characterization of the materials

To process the data obtained from the breaking-thread experiments, the knowledge of the zero shear viscosity, η_0, of each of the components is required at the measurement temperature. Measurements were performed on a constant stress rheometer (Rheometrics DSR) in plate–plate configuration (plate radius 25 mm). Experimental data at low shear rates ($\dot{\gamma} < 0.01\ \mathrm{s}^{-1}$) were obtained from creep tests; oscillatory experiments provided dynamic viscosities at frequencies between 0.01 and 10 rad/s. The dynamic data were fitted according to a modified Cross model (Eq. (7)) to extrapolate the value of η_0 [32].

$$\eta = \eta_0 + [1 + |a\dot{\gamma}|^m]^{-1}. \tag{7}$$

In Eq. (7), η_0 is the zero shear viscosity (in Pa s), $\dot{\gamma}$ is the shear rate (in s^{-1}), a is a fitting constant, and m is the power law constant. Thus, the obtained values for η_0 proved to be comparable with the results of the creep tests.

Samples for the rheological measurements were prepared by compression molding the dried materials into discs with a diameter of 25 mm and a thickness of 1–1.5 mm. Temperatures at which the samples were compression molded were typically 40–50°C above the melting point of the semicrystalline polymers (PP12, PP40 and POM), or 90–100°C above the glass transition temperature of the amorphous polymers (PS, PS/PPE blends).

2.3.4. Capillary instability observations

Threads of the amorphous PS/PPE blends were drawn from a molten granule on a hot plate. Thread diameters were typically in the range of 10–50 μm, and were dependent on the expected break-up times which should be preferentially between 2 and 10 min in order to avoid degradation. All matrix polymers were compression molded at 230°C into thin films (thickness ±150–200 μm).

Measurement samples were prepared by positioning some threads between two films of a matrix polymer, taking care that a minimum of contamination was included. The whole structure was consolidated between a glass slide and a cover glass and placed in a hot stage (Mettler FP-90). The thread was visualized by a Nikon optical microscope equipped with a Sony CCD-camera, thereby allowing to record break-up images on a video with internal timer. Prior to the break-up experiments, the samples were heated at 20°C/min to a temperature slightly above the melting point, T_m, of the matrix film and kept there for at least

Table 3
Zero shear viscosity, η_0, of the materials used for the capillary instability experiments

Material	Temperature (°C)	η_0 (Pa s)
PP-12	220	2450
	230	1425
	245	1140
PP-40	230	250
PS	220	2250
	230	1453
PS/PPE 100/0 (Hal)	220	1260
	230	792
PS/PPE 90/10 (Ha3)	230	1790
PS/PPE 75/25 (Ha5)	230	6615
	245	2817
PS/PPE 50/50 (Ha7)	230	62 000
POM	220	1900
	230	1565

1 min, in order to allow the matrix polymer to flow around the thread equally, and to avoid air inclusions at the fiber/matrix interface. Subsequently, the sample was heated quickly to the measuring temperature. An image processing system (Visilog 4.1.3.) was used to measure the initial thread diameter, $D_0 = 2R_0$, the distortion amplitude, α (Eq. (8)), and the wavelength, λ, of the growing distortions.

$$\alpha = \frac{(D_{\max} - D_{\min})}{4}. \tag{8}$$

From a plot of the experimental value $2\alpha/D_0$ versus time on a semi-logarithmic scale, the growth rate of the capillary instabilities, q, can be determined from the slope of the curve (Fig. 3). The value of the interfacial tension in the system was then calculated according to Eq. (3).

For each system, at least six experiments were performed to be able to calculate a more or less reliable statistical average of the interfacial tension in the system.

2.4. Results of the breaking-thread measurements

2.4.1. Rheological properties of the materials

The zero shear viscosities, η_0, of the materials, as extrapolated from a modified Cross model, are listed in Table 3 for each temperature.

An overview of the shear rate-dependent flow behavior at 230°C is given in Fig. 4(a) for the semicrystalline matrix materials, and in Fig. 4(b) for the amorphous PS/PPE threads. As the POM samples suffered seriously from degradation during the rheological measurements, a new sample for each creep test had to be used, and only the first few data points obtained during oscillation experiments were found to be reliable. All the thread polymers showed Newtonian flow behavior in the low frequency region ($f < 0.1$ rad/s). A similar behavior was observed for the matrix materials PP40 and POM. For the PP12, the Newtonian plateau at low frequencies was less obvious. Measurements performed at different temperatures were extrapolated by means of an Arrhenius equation to estimate the activation energy, E_a, of this polypropylene. A value of 63 kJ/mol was found, which corresponds reasonably with the value of 84 kJ/mol measured on another commercial PP sample [33].

2.4.2. Interfacial tension, σ_{12}, in PP/(PS/PPE) and POM/(PS/PPE) systems

A standard measuring temperature of 230°C was chosen for the majority of the breaking-thread experiments. At this temperature, the matrix materials (PP or POM) do not suffer too much from degradation, the zero shear viscosity of all materials is still easily measurable, and the threads are well above their flow temperature to allow break-up within reasonable time scales. A limited amount of experiments were conducted at other temperatures to verify the reproducibility of the values and to have an idea on the temperature dependence of the interfacial tension, σ_{12}.

Table 4 summarizes the experimental data for the interfacial tension on each system with PP as the matrix material. The data for blend systems with POM are listed in Table 5. For the calculation of σ_{12}, only those results of thread break-up which occurred at a wavenumber, X, deviating not more than ±10% from the dominant wavenumber, X_m were taken into account. Luciani et al. [26] demonstrated that the value of the growth rate function $\Omega(X,p)$ in such a case does not deviate too much from $\Omega(X_m,p)$. This is certainly the case for our investigated systems, all having a viscosity ratio, p, larger than 0.5, where the function $\Omega(X,p)$ changes only slightly (Fig. 2).

The interfacial tension of the *PP/Ha7 system* could not be measured via the capillary break-up method. At a standard measuring temperature of 230°C, no break-up could be observed even after 120 min. Luciani et al. [26] encountered similar difficulties for systems with highly viscous materials and stated that the method was only suited to systems in which the components have a zero shear viscosity below the 30–40 kPa s range, which is indeed not fulfilled in this case. A theoretical estimate of the thread diameter yielding reasonable break-up times at 230°C can be obtained from Eq. (6). If a value for σ_{12} of roughly 5 mN/m is assumed, the time for thread break-up can be calculated with $\eta_m = 1425$ Pa s, $p = 43.5$, $\Omega_m = 0.00586$, and $T = 503$ K. For a thread with an initial diameter D_0 varying from 10 to 50 μm, the calculated break-up times were of the order of 50–300 min, which confirms with our experimental results. Due to the high viscosity of the material, the preparation of thinner threads that would break up faster is quasi impossible.

Experiments at a higher temperature (250°C) did only partially result in normal thread break-up; most threads showed a quite irregular behavior and often a combination of break-up and thread relaxation could be observed. The latter is probably related to the non-Newtonian behavior at low shear rates and the high elasticity of the PS/PPE 50/50 melt. Experiments at even more elevated temperatures probably would solve the problem of thread break-up, but are

Table 4
Interfacial tension as determined by the capillary thread break-up method

Thread	T (°C)	D_0 (μm)	X_{exp}	q ($\times 10^{-3}$ s^{-1})	σ_{12} (mN/m)
(a) For PP12 systems					
PS	230	24.12	0.561	10.385	4.96
		46.65	0.543	6.78	6.27
$p = 1.02$		23.32	0.567	12.12	5.60
$X_m = 0.564$		29.87	0.552	10.59	6.27
$\Omega_m = 0.0719$		29.37	0.423	8.93	5.20
		29.37	0.572	9.00	5.24
Average			0.54		**5.6** ± 0.5
Ha1	230	32.06	0.536	10.57	5.09
		33.70	0.484	11.40	5.77
$p = 0.556$		45.49	0.520	9.58	6.54
$X_m = 0.583$					
$\Omega_m = 0.0949$					
Average			0.51		**5.8** ± 0.5
Ha3	230	29.51	0.579	11.61	7.20
		29.51	0.618	10.22	6.58
$p = 1.256$		23.89	0.463	9.68	5.04
$X_m = 0.556$		16.81	0.531	18.87	6.92
$\Omega_m = 0.0653$		32.70	0.581	8.95	6.39
Average			0.55		**6.4** ± 0.7
Ha5	230	28.44	0.416	3.61	4.56
		28.14	0.577	5.26	5.84
$p = 4.64$		25.31	0.425	3.69	4.15
$X_m = 0.476$					
$\Omega_m = 0.0321$					
Average			0.47		**4.9** ± 0.7
Ha5	245	31.32	0.394	6.22	4.76
		24.66	0.337	6.91	4.16
$p = 2.47$		17.69	0.327	11.00	4.75
$X_m = 0.52$		38.52	0.403	4.60	4.33
$\Omega_m = 0.0467$		13.67	0.469	14.81	4.95
		33.00	0.471	6.72	5.41
		29.76	0.445	6.97	5.07
Average			0.41		**4.8** ± 0.4
(b) For PP40 systems					
PS	230	52.72	0.472	10.04	4.78
		59.37	0.429	9.94	5.33
$p = 5.81$		46.50	0.417	10.22	4.29
$X_m = 0.458$		45.40	0.475	14.54	5.96
$\Omega_m = 0.0277$		49.07	0.470	10.39	4.54
Average			0.45		**5.0** ± 0.5

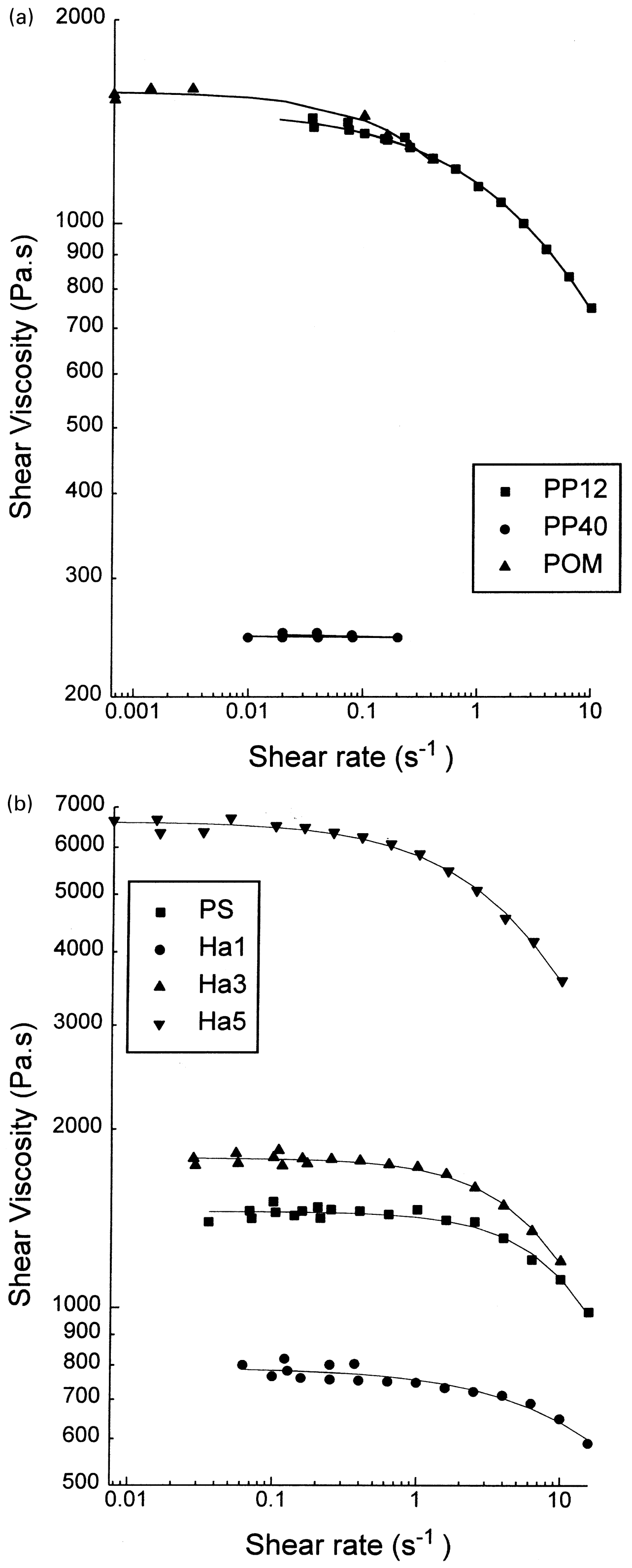

Fig. 4. Shear viscosity versus shear rate at 230°C as measured by a plate–plate rheometer for: (a) semicrystalline matrix materials, and (b) amorphous thread materials.

practically of no use. Higher temperatures would cause polymer degradation during the measurements, hence influencing the growth rate of the distortions (and thus σ_{12}); additionally, the determination of the zero shear viscosity would become highly erroneous due to material degradation. A global overview of all results is given in Table 6.

The results obtained at 230°C can be graphically evaluated from Fig. 5. A linear regression analysis of the interfacial tension versus PPE content confirms that the interfacial tension between PS/PPE mixtures and PP or POM are virtually independent of the PS/PPE blend ratio. The calculated value for the slope $\Delta = d(\sigma_{12})/d(\%PPE)$ was 0.031 ± 0.031 for PP/(PS/PPE) systems and 0.050 ± 0.049 for POM/(PS/PPE) systems, and can thus be considered as negligible. Moreover, if the less reliable results obtained for PP12/Ha1 and POM/Ha1 systems are not taken into

Table 5
Interfacial tension as determined by the capillary thread break-up method for POM systems

Thread	T(°C)	D_0 (μm)	X_{exp}	q ($\times 10^{-3}$s^{-1})	σ_{12} (mN/m)
PS	230	30.52	0.560	13.33	8.39
		22.64	0.569	21.01	9.81
$p = 0.928$		29.54	0.561	17.40	10.60
$X_{\mathrm{m}} = 0.567$		37.18	0.596	12.02	9.21
$\Omega_{\mathrm{m}} = 0.0759$		28.29	0.485	17.84	10.41
Average			0.56		**9.7** ± 0.7
PS	220	32.51	0.584	12.18	11.20
		32.17	0.562	11.45	10.53
$p = 1.184$		47.53	0.614	5.414	7.28
$X_{\mathrm{m}} = 0.5585$		31.35	0.623	12.03	10.67
$\Omega_{\mathrm{m}} = 0.0672$					
Average			0.59		**9.9** ± 1.4
Ha1	230	35.90	0.538	24.94	14.14
		74.40	0.519	6.67	7.84
$p = 0.506$		60.41	0.581	12.69	12.11
$X_{\mathrm{m}} = 0.585$		27.40	0.574	28.60	12.38
$\Omega_{\mathrm{m}} = 0.0991$		28.65	0.532	31.25	14.14
		91.65	0.640	4.06	5.88
Average			0.56		**11.1** ± 1.7
Ha5	230	22.30	0.495	10.07	10.30
		22.30	0.430	9.07	9.28
$p = 4.23$		51.01	0.517	4.18	9.78
$X_{\mathrm{m}} = 0.482$		37.55	0.481	4.99	8.60
$\Omega_{\mathrm{m}} = 0.0341$		32.50	0.524	5.63	8.40
		27.65	0.543	6.41	8.14
Average			0.50		**9.1** ± 0.7

consideration, the interfacial tension clearly remains unaffected by varying concentrations of PPE in the PS/PPE phase. PP12/Ha1 and POM/Ha1 blend systems showed some difficulties during break-up measurements, because the Ha1 thread started softening nearly at the same temperature as the PP12 and POM matrix film; as such, the embedding of the fiber can be somewhat disturbed. As a consequence, a slightly compressed thread will yield overestimated values for the initial thread diameter, and hence a highly erroneous interfacial tension. Attempts to use Ha1 as a matrix film with PP or POM as the thread component turned out to be even worse, because the fiber could not be embedded properly by the amorphous Ha1 film.

3. Pendant drop analysis

3.1. Theory

Pendant drop analysis (PDA) is one of the most widely used equilibrium methods to measure the interfacial tension. It has been used in many studies of polymeric systems, often with low molecular weight materials [11,13,30,34–37]. The technique is based on the analysis of the equilibrium shape of a drop of component 1 emerging from a capillary [35]. This drop can be immersed in component 2 for interfacial tension measurements, or in an inert atmosphere for surface tension determination.

The difference in pressure Δp at the curved interface is linked to the interfacial tension, σ_{12}, by the Young–Laplace equation (Eq. (9)), with R_1 and R_2 the principal radii of curvature of the interface (Fig. 6)

$$\Delta p = \sigma_{12}\left(\frac{1}{R_1} + \frac{1}{R_2}\right). \tag{9}$$

The equilibrium profile of a pendant drop can be expressed by the dimensionless set of differential equations (Eq. (10)) (Fig. 6):

$$\frac{\mathrm{d}\Phi}{\mathrm{d}s} = \frac{2}{B} - Z - \frac{\sin\Phi}{X},$$

$$\frac{\mathrm{d}X}{\mathrm{d}S} = \cos\Phi \qquad \frac{\mathrm{d}Z}{\mathrm{d}S} = \sin\Phi. \tag{10}$$

With the boundary conditions at the drop apex [38,39]:

$$X(0) = Z(0) = \Phi(0) = 0$$

$$(\sin\Phi)X = 1/B$$

where the dimensionless shape factor, B, is defined as:

$$B = R_0\left(\frac{\Delta\rho g}{\sigma_{12}}\right) \tag{11}$$

with $\Delta\rho$ the density difference between the two components (in g/cm^3); g the gravity constant ($= 9.81$ m/s^2); and R_0 the radius of curvature at the drop apex ($R_0 = R_1 = R_2$).

Table 6
Overview of the results of interfacial tension measurements at 230°C via the breaking-thread method according to the theory of Tomotika

Film/thread	Temperature (°C)	Viscosity ratio $\eta_{\mathrm{d}}/\eta_{\mathrm{m}}$	Average σ_{12} (mN/m)	Standard deviation (mN/m)	% error	X_{m} theor.	X_{exp}
PP12/PS	230	1.0	5.6	0.5	8.2	0.564	0.54
PP12/Ha1	230	0.6	5.8	0.5	8.5	0.583	0.51
PP12/Ha3	230	1.3	6.4	0.7	10.3	0.556	0.55
PP12/Ha5	230	4.6	4.9	0.7	13.6	0.476	0.47
PP12/Ha5	245	2.5	4.8	0.4	7.5	0.520	0.41
PP40/PS	230	5.8	5.0	0.5	10.6	0.458	0.45
POM/PS	230	0.9	9.7	0.7	7.3	0.567	0.56
POM/PS	230	1.2	9.9	1.4	14.1	0.559	0.59
POM/Ha1	230	0.5	11.1	1.7	15.5	0.585	0.56
POM/Ha5	230	4.2	9.1	0.7	7.7	0.482	0.50

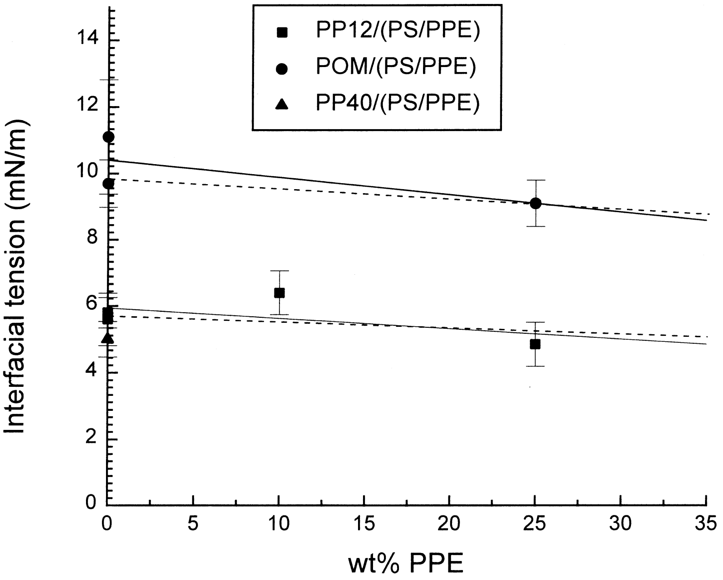

Fig. 5. Influence of the PPE content in PS/PPE mixtures on the interfacial tension in systems with PP or POM, as measured from breaking thread experiments; full lines fit all data points, dashed lines exclude data points with systems containing Ha1.

Using this system of equations, the surface tension of a pendant drop can be estimated by comparing the experimental drop profile with theoretical profiles calculated from the Young–Laplace equation (Eq. (9)). From Eq. (11), it is obvious that an accurate knowledge of the densities of each material at the measuring temperature, together with a very precise shape analysis of the formed pendant drop is an absolute condition for reliable results of the surface tension, σ, and the interfacial tension, σ_{12}.

3.2. Advantages and limitations of pendant drop analysis

PDA is a static method suited to determine both the surface tensions of polymeric melts and the interfacial tension between two polymeric materials in the melt state. Measurements require a highly specialized apparatus set-up. Contrary to breaking thread experiments, which are based on the knowledge of the zero shear viscosity, η_0, PDA requires the accurate knowledge of the density of the materials at each measuring temperature. Measurements often last at least half an hour because the drop shape analysis has to be performed on fully equilibrated and stable pending droplets. This implies that the method becomes inapplicable in all cases where polymer degradation can be expected, or if one of the components is highly viscous and/or elastic. Further, the method is also difficult for low viscous materials which tend to fall off the syringe, rather than forming a stable pending droplet. The best results generally are obtained for systems with a viscosity ratio, p, between 0.1 and 1.

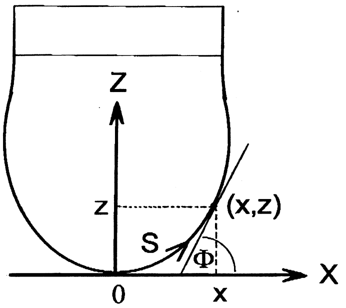

Fig. 6. Drop shape analysis parameters as used for the determination of the interfacial tension in the PDA technique.

3.3. Experimental

3.3.1. Materials

PDA experiments have been performed to estimate the influence of the PPE content in amorphous homogeneous PS/PPE mixtures, both on the surface tension of the PS/PPE blends and on the interfacial tension of PP/(PS/PPE) blends. The amorphous materials used are a commercial PS, Styron® E680, from Dow Benelux N.V. (Table 1), and the PS/PPE mixtures which have been described previously (Table 2). The polypropylenes used in these experiments were a commercial PP12 supplied by Atochem (Table 1) and a Hostalen® PPT 1070 polypropylene (PP5) from Hoechst AG, with a higher melt viscosity than the PP12 (MFI 230°C = 5 g/10 min; $M_w = 226\ 000$ g/mol; $M_n = 44\ 600$ g/mol).

3.3.2. Determination of the density data

Densities at 25°C were determined by means of an Ultrapycnometer 100 (Quantachrome) equipped with a 50 cm^3 pycnometer cell. Helium was used as a test gas. The polymeric material was studied in the form of small granules. The accuracy is found to be better than 0.03 %.

The dependence of the density of the molten polymers on

Table 7
Density of materials as extrapolated from *pVT* measurements in the melt and as determined from Helium pycnometer tests at 25°C

Material	Density function[a]			Density at 25°C (g/cm^3)
	Intercept (*A*)	Slope (*B*)	Temperature range (°C)	
PP12	0.85492	− 0.0005501	180–256	0.8831
PP5	0.85845	− 0.0005360	193–299	0.903
PS	1.08895	− 0.0005851	196–271	1.0535
PS/PPE 90/10 (Ha3)	1.11274	− 0.0006244	196–272	1.061
PS/PPE 75/25 (Ha5)	1.11715	− 0.0006216	202–278	1.0693

[a] $\rho(T) = A + BT$(°C) in g/cm^3. (Note that the density of a polymer melt is not linearly dependent on temperature; the calculated density function is thus only valid in the temperature range indicated here)

the temperature was calculated from the *pVT* data of the polymer melts obtained by means of a GNOMIX PVT-Apparatus (GNOMIX). The *pVT* data were collected in the isothermal standard mode (ITS) in the temperature range from room temperature to about 25 K above the highest temperature at which PDA was carried out, in steps of 15 K. The pressure varied from 10 to 200 MPa in steps of 10 MPa. The specific volume at atmospheric pressure was extrapolated from these data for each temperature by the GNOMIX *pVT* software. The accuracy of the specific volume data is ±0.002 and ±0.004 cm^3/g at temperatures up to 250°C or above 250°C, respectively. Finally, a linear dependence of the densities on temperature is assumed within the temperature range of PDA measurements.

3.3.3. Surface and interfacial tension measurements

The surface and interfacial energy data were obtained by means of a pendant drop apparatus. This selfmade apparatus (Institute of Polymer Research, Dresden, Germany) consists of a NRL contact angle goniometer (Ramé–Hart, Inc.) equipped with an optical bench, illuminator and microscope, an environmental chamber with temperature controller, a heatable syringe attachment, a video camera (Sony XC 77CE), and an RGB monitor (Sony PVM 1442 QM). A weak argon flow is conducted through the environmental chamber. The temperature of both the environmental chamber and the syringe can be controlled to within 1°C, in a temperature range from room temperature to 344°C. The apparatus is controlled by a personal computer (IBUS PC Technologies), equipped with a frame grabber (ITI OFG-KIT-C2-AT), image analysis software (BioScan Optimas V 3.01) and drop shape analysis software (DSA, Kriss, Germany) based on the algorithm developed by Song and Springer [40]. The drop shape analysis was performed in three steps. Firstly, the drop image has to be digitised; from this drop image a binary drop profile can be extracted; finally, a curve fitting program compares the experimental drop profile with theoretically calculated profiles according to the Young–Laplace equation (Eq. (9)). For polymer melts, the reproducibility of the method is within ±0.3 mN/m for the surface tension and within ±0.6 mN/m for the interfacial tension.

Table 8
Surface tensions measured by the PDA in argon atmosphere and extrapolated surface tension functions for the amorphous melt of all materials

Material	Temperature PDA (°C)	σ (mN/m)	Function $\sigma(T) = A + B\,T$ (°C)	
			Intercept (*A*)	Slope (*B*)
PP12	210	19.4		
	230	18.2	30.8	− 0.054
	250	17.3		
PP5	250	17.8	28.1	− 0.041
	260	17.4		
PS	220	27.6		
	245	25.8	42.3	− 0.067
	265	24.6		
PS/PPE 90/10	230	26.7		
	250	25.7	39.1	− 0.054
	265	24.8		
PS/PPE 75/25	240	26.2		
	255	26.1	35.2[a]	− 0.036
	270	25.5		

[a] Linear regression without data point at 240°C because of its rather uncertain nature (rather high viscosity at lower temperatures, leading to long equilibration times and risk for degradation).

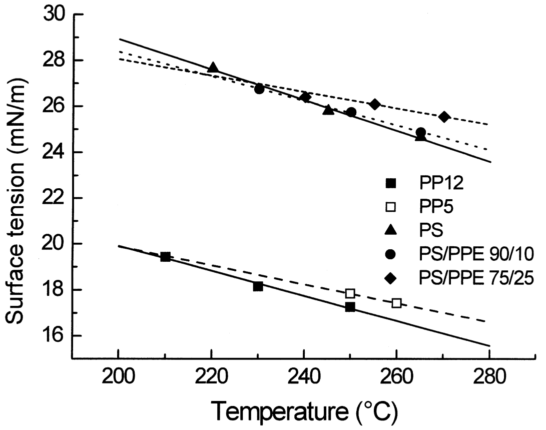

Fig. 7. Experimentally determined surface tensions from PDA as a function of temperature; full lines indicate the linearly fitted surface tension functions.

3.4. Results of the pendant drop analysis

3.4.1. Density of the materials

The density of the used solid polymers determined at room temperature (25°C), and the temperature-dependent linear density functions of the polymer melts are listed in Table 7.

From the density functions, the exact density of each material at the PDA measuring temperature can be calculated. The density of the PS/PPE mixtures was found to be influenced only slightly by the PPE content.

3.4.2. Surface tensions of the amorphous melts

The surface tensions of all materials measured by the PDA are listed in Table 8.

A linear regression on the experimental data with respect to temperature yields a (linear) surface tension function, $\sigma(T)$. The latter gives a good idea of the temperature dependence for each material within the temperature region under investigation (Fig. 7).

In the temperature region of our interest (260°C), the influence of the content of PPE in the PS/PPE mixtures on their surface tension seems to be negligible. The observed difference of $\sigma(260°\text{C})$ with about 1 mN/m is of the same order of magnitude as the experimental error of the measurements.

Measurements on a PS/PPE mixture containing 50 wt.% PPE turned out to be impossible because of its extremely high viscosity, even at elevated temperatures; no equilibrium drop shape could be formed within a reasonable time scale.

Table 9
Experimental data of the interfacial tension measured by PDA

System	wt.% PPE	T (°C)	σ_{12} (mN/m)
(a) PP12/(PS/PPE) systems			
PP12/PS	0	225	4.8
PP12/Ha3	10	225	4.6
PP12/Ha5	25	230	5.9
		240	5.2
(b) Hostalen® PPT 1070/(PS/PPE) systems			
PP5/PS	0	225	4.6
		240	4.7
PP5/Ha3	10	230	5.3
		240	5.5
		250	5.6
PP5/Ha5	25	240	6.1
		250	6.0
		260	6.2

3.4.3. Interfacial tension in PP/(PS/PPE) blend systems

Measurements of the interfacial tension in PP/(PS/PPE) systems were always performed by analyzing the shape of a higher density PS/PPE droplet immersed in a less density PP melt. The latter set-up proved to be the best way to reach a smoothly equilibrated droplet shape. The temperature of each measurement was adjusted depending on the viscosity of the droplet material. The results of all measurements are listed in Table 9. The error in the measurements is of the order of ±0.6 mN/m.

Measurements with the lower viscous PP12 posed some difficulties; some small air bubbles entrapped within the granules were difficult to remove from the melt and disturbed the normal formation of an equilibrium droplet. Only a limited amount of data points were measured. To solve this problem, a parallel series of measurements was carried out with a Hostalen® PPT 1070 (PP5) as the matrix melt. The latter has a somewhat higher melt viscosity than PP12. Also this polymer caused some difficulties during the necessary long equilibration times for drop formation; inhomogeneities were sometimes visible. However, measurements of the interfacial tension versus PS yielded approximately the same results as obtained in a PP12 matrix melt. Hence, it was assumed that the data obtained with both types of PP could be compared. An overview of all experimental data is given in Fig. 8.

4. Discussion

The effect of PPE in PS/PPE mixtures on the surface tension and on the interfacial tension in PP/(PS/PPE) systems was evaluated both from the dynamic breaking thread method, and from an equilibrium method called the pendant drop analysis. To confirm the observed tendencies, some supplementary measurements of σ_{12} were performed for a POM/(PS/PPE) system by the breaking thread method.

The results of both the pendant drop analysis and the breaking thread method were in agreement with each other for the PP12/(PS/PPE) system. The interfacial tension measured for PP12/PS around 230°C was found to be of the order of 4.5 to 5.5 ± 0.6 mN/m. These values are well within the range of the previously reported data in literature (Table 10).

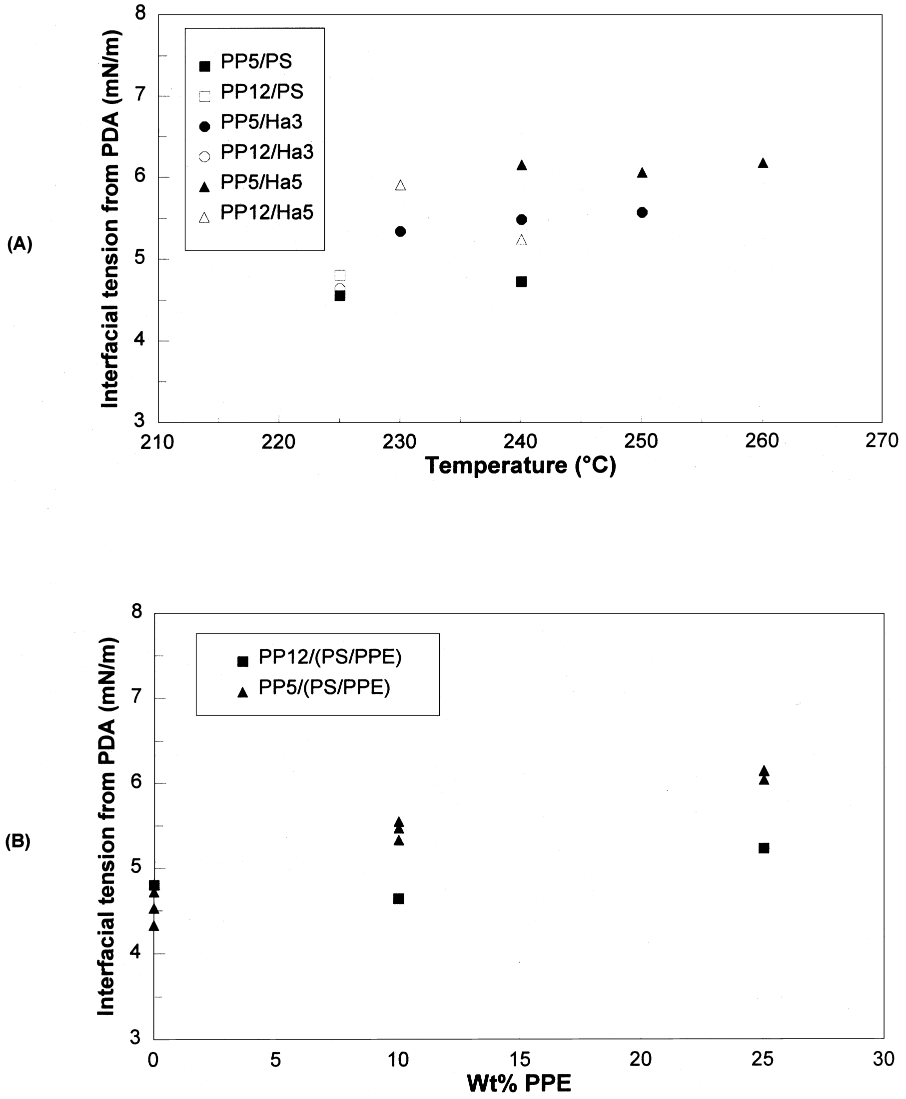

Fig. 8. Interfacial tension in PP/(PS/PPE) systems measured by PDA: (a) as a function of temperaure; and (b) as a function of the PPE content in the PS/PPE phase.

Table 10
Literature data on the interfacial tension in PP/PS

Temperature (°C)	σ_{12} (mN/m)	$-\Delta\sigma_{12}/\Delta T$	Reference
150	5.1	–	Polymer Handbook [49]
			Oda and Hata [41]
185	5.25	0.011	Nemirovski et al. [42]
220	4.9		
226	3.1	0.015	Demarquette and Kamal [43]
250	3.5		Kamal et al. [44]
220	5.8		
235	4.9	0.07	Escudie et al. [34]
250	3.7		
300	5.0	–	Machiels et al. [27]
225	4.5	0.008	Pionteck [45]
250	4.3		

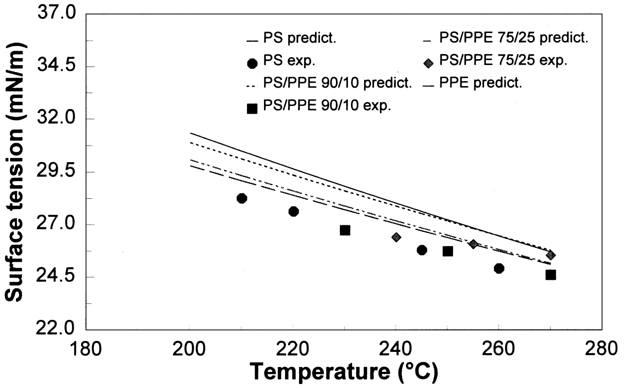

Fig. 9. Comparison of the surface tension to PS/PPE mixtures as predicted from Eq. (12), with the experimentally determined data points from PDA.

4.1. Influence of the PPE content in PS/PPE on the surface tension

The *influence of PPE* in PS/PPE mixtures on the *surface tension* was investigated based on the (PDA) experiments. The high melt-viscosity of the PS/PPE mixtures containing more than 25 wt.% of PPE, resulting in long equilibration times and consequently thermal degradation of the polymers, restricted the applicability of PDA to only a small part of the composition range of the PS/PPE mixtures. The absolute value of the surface tension, $\sigma(T)$, in the temperature range under investigation (200–260°C) was found to remain nearly constant for all compositions around 26 ± 1 mN/m. It can thus be concluded that PPE does not affect the surface tension of the PS/PPE mixtures significantly. Note the slightly deviating temperature dependence of the surface tension of PS/PPE mixtures containing higher amounts of PPE. This can possibly be attributed to the lower reliability of the PDA measurements in more elastic and/or viscous systems where the polymer melt does not readily attain its equilibrium shape, leading to more erroneous results at low temperatures.

A *theoretical* estimation of the influence of PPE on the *surface tension* of the PS/PPE mixtures can be performed from Macleod's relationship between the surface tension, $\sigma(T)$, and the density of the material (Eq. (12)), as the exact densities of all our materials were measured for the PDA experiments.

$$\sigma_i = \left(\frac{P}{M1}\right)^{\beta} \rho^{\beta}, \tag{12}$$

where P is the Sugden Parachor for a repeating unit (cm^3/mol)(mJ/m^2)$^{1/4}$, values are listed by Van Krevelen [46], $M1$ is the molecular weight of a repeating unit (g/mol), β is the Macleod's constant, and ρ is the temperature-dependent density of the material (g/cm^3). The values of P, $M1$ and β are independent of temperature.

For the estimation of the surface tension of PS and PPE from Eq. (12), the following values were used: $M1(\text{PPE}) = 120$, $M1(\text{PS}) = 104$ g/unit/mol; and $P(\text{PPE}) = 269$, $P(\text{PS}) = 250$. The Macleod's constant has been assumed to be the same for both PS and PPE; a value of 4.0 reported for PS [49] was used for the calculations. The exact density of the polymers as a function of temperature was calculated from the extrapolated density functions listed in Table 7. The density of pure PPE in this temperature range was estimated on the basis of the density functions of PS/PPE mixtures. The results of this theoretical estimation from Eq. (12) were compared with the experimental results obtained from PDA measurements (see Table 8) and are represented in Fig. 9.

A slight increase of the surface tension of only 1–2 mN/m with increasing PPE content was predicted from Macleod's relationship (Eq. (12)). For PS/PPE mixtures with a PPE content as low as 25 wt.%, this deviation thus becomes rather irrelevant. The experimental error of the PDA measurements is even larger than the calculated change of the surface tension in the PS/PPE mixtures. Hence, it may be concluded that the surface tension in PS/PPE mixtures indeed is not affected at all over the whole composition range.

This may also be confirmed by the scarce experimental data for the surface tension of PS/PPE mixtures reported in the literature. For a commercial PS/PPE 30/70 mixture, a value of 30.8 mN/m was measured by the dynamic contact angle analysis [47]. This value is very close to the values reported in the literature for pure PS [30], and the values determined experimentally by PDA for Styron® PS E680, and is in agreement with the predicted value of $\sigma(T)$ from Eq. (12).

4.2. Influence of the PPE content in PS/PPE on the interfacial tension in PP/(PS/PPE) and POM/(PS/PPE) systems

The *effect of the PPE content* in the PS/PPE mixtures on the *interfacial tension* in a PP/(PS/PPE) system was measured for two types of PP matrix material.

The interfacial tension as measured in systems with PP12 did not seem to be influenced much by changing the content of PPE in the PS/PPE phase, at least for compositions containing up to 25 wt.% PPE. This tendency is also found in the POM/(PS/PPE) systems from capillary instability observations. Similar results were obtained from spinning drop experiments by Schoolenberg [48]. Measurements were performed for the interfacial tension between PS/PPE mixtures, and PP (commercial Shell grade, $\rho_{(25°\text{C})} = 0.905$ g/cm^3) and PE (lab grade LLDPE, $\rho_{(25°\text{C})} = 0.920$ g/cm^3, $\eta_{240°\text{C}} = 307$ Pa s), respectively. The PS/PPE mixtures used in the test were a PS ($\rho_{(25°\text{C})} = 1.04$ g/cm^3) and PS/PPE 50/50 (Noryl®, $\rho_{(25°\text{C})} = 1.06$ g/cm^3) supplied by the General Electric. The interfacial tension values of PP/PS and PE/PS were found to be both around 4.5–4.7 mN/m at 240°C, whereas the value of σ_{12} for systems of PP/Noryl® and PE/Noryl® was only 0.4 mN/m lower. Taking into account the error on such

Table 11
Polarity, x_p, of the basic materials extrapolated from literature data

Material	Extrapolated x_p	Literature data
PP	0.02	0.02
PS	0.17	0.17
PS/PPE 90/10	0.173	
PS/PPE 75/25	0.177	
PS/PPE 50/50	0.183	
PS/PPE 70/30	0.188	0.188 [47]
PPE	0.20	

measurements, it can be concluded that the content of PPE in the PS/PPE mixtures does not affect the interfacial tension.

In the case of systems with PP5, a slight increase of the interfacial tension with increasing content of PPE in the region of 220–260°C can be observed. This observation is not in line with all other measurements, and probably can be assigned to the not yet equilibrated droplet shape. A more viscous matrix causes a slowly developing droplet shape; if drop shape analysis is performed on not fully equilibrated droplets, the measurements become highly erroneous.

To judge the evolution of the interfacial tension in PP/(PS/PPE) systems with increasing content of PPE in the PS/PPE mixture in a more reliable way, σ_{12} can be *predicted directly* by using the theoretically calculated surface tension functions for PS/PPE mixtures predicted from Macleod's theory (Fig. 9) in the *harmonic mean equation* [30]:

$$\sigma_{12} = \sigma_1 + \sigma_2 - 4\frac{\sigma_1^{d}\sigma_2^{d}}{\sigma_1^{d} + \sigma_2^{d}} - 4\frac{\sigma_1^{p}\sigma_2^{p}}{\sigma_1^{p} + \sigma_2^{p}}, \qquad (13)$$

where σ_i is the surface tension (mN/m), x_p the polarity of component i; σ_i^p the polar component of σ_i, $\sigma_i^p = x_p\sigma_i$; and σ_i^d the dispersive component of σ_i, $\sigma_i^d = (1 - x_p)\sigma_i$.

The knowledge of the *polarity* of PP, PS and PPE is required for such calculations. The polarity of PP and PS is listed in the literature [49] as 0.02 for PP and 0.17 for PS. These values are independent of temperature [30]. As no literature data are available on the polarity of PPE, an estimation was made based on the polarity of PS/PPE 30/70 reported in literature (Table 11). Crevecoeur [47] determined the surface tension of PS/PPE 30/70 using the dynamic contact angle analysis. A value of 30.8 mN/m was measured; 5.8 mN/m was attributed to the polar component, $\sigma^p = x_p\sigma$. From the value of σ^p, the polarity in PS/PPE 30/70 was found to be 0.188. Assuming that the contribution of PPE to the polarity of the mixture is a linear function of the content of PS and PPE, the polarity in such mixtures can be estimated from Eq. (14) and is listed in Table 11. Calculations indicate a quasi-negligible change of the polarity in the PS/PPE mixtures with increasing amount of PPE

$$x_p = x_p(\mathrm{PS}) + \frac{\%\mathrm{PPE}}{70}[x_p(\mathrm{PS/PPE30/70}) - x_p(\mathrm{PS})]. \qquad (14)$$

The estimated interfacial tension, calculated via the harmonic mean equation (Eq. (13)) is presented in Fig. 10.

From the latter calculations, it can be seen that the interfacial tension in PP/(PS/PPE) remains quasi constant around 5.0 mN/m, at least for PS/PPE mixtures with a PPE content not exceeding 25%. The total predicted change in σ_{12} over the whole composition range is only 1 mN/m, which approximates the experimental error on both the PDA and the breaking thread measurements.

The tendency observed from the calculated interfacial tension functions (Fig. 10) agrees with the experimentally observed behavior for PP12/(PS/PPE), except for PP/Ha5 systems. It can thus be concluded that PDA with more viscous polymeric material leads to less reliable results. The temperature dependence of the interfacial tension is predicted to be around −0.01 mN/m K, which is also consistent with the literature data [30,50].

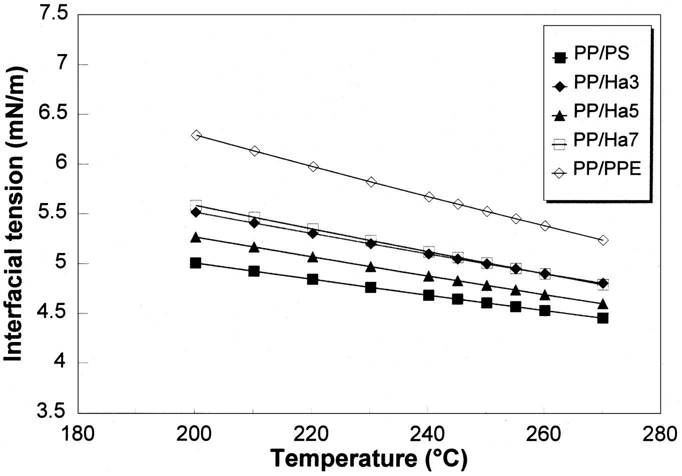

Fig. 10. Predicted evolution of the interfacial tension in PP/(PS/PPE) systems via the harmonic mean equatioin, based on surface tension functions calculated from Macleod's relationship.

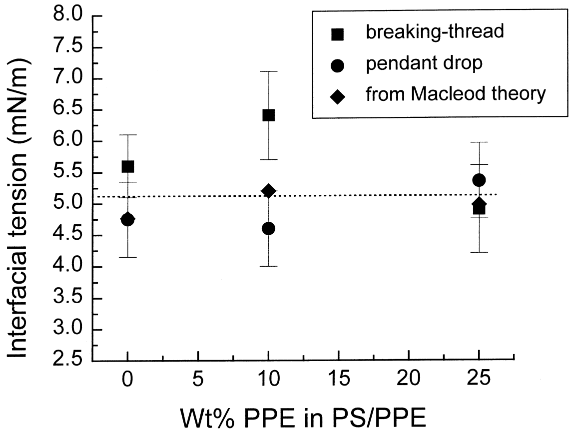

Fig. 11. Comparison of the interfacial tension at 230°C in PP12/(PS/PPE) systems determined experimentally from the breaking thread and PDA with values predicted via the harmonic mean equation based on surface tension functions obtained from Macleod's theory.

4.3. *Comparison of methods*

To evaluate the relevance of our experimentally determined interfacial tensions, the data obtained at 230°C from the breaking thread experiments and the PDA were plotted along with the theoretically calculated values of σ_{12} from the surface tensions predicted by the Macleod theory (see Fig. 10) in Fig. 11.

The general tendency of the measured data and calculated values indicate that the interfacial tension in PP/(PS/PPE) system is rather insensitive to the PPE content.

From the experimentally determined data, it can be seen that both the PDA and the breaking thread method suffer from a significant standard deviation, leading to rather widely scattered results. It should be pointed out, however, that the error on data from the breaking thread measurements is significantly higher than that on data obtained via PDA. The displayed error bars on the breaking thread measurements are a result of at least six experiments from which the worst results (i.e. when X_{exp} differs more than 10% from X_{m}) were already eliminated before further calculations were performed. Further, droplet break-up, in practice, never occurs exactly at the dominant wavelength predicted by the theory of Tomotika (Fig. 2); elastic effects can cause faster disruption of the liquid thread cylinders leading to highly erroneous capillary instability growth rates, thread preparation methods never ensure a fully controlled and equal thread diameter over the entire length under investigation, etc. In contrast to the breaking thread experiments, the PDA involves less external factors that can give rise to experimental errors. Once the conditions of a fully equilibrated, not degraded pendant drop are achieved, drop shape analysis can be performed in a straightforward manner. The general error accepted for the PDA experiments is of the order of ± 0.6 mN/m for each measurement, whereas a similar value is found for on an average six breaking thread experiments.

It should, however, be mentioned that the PDA method is, as a consequence of its absolute precondition of equilibrium state, limited to a narrow range of measurement temperatures and material viscosities. The breaking thread measurements offer the possibility for the experimental determination of σ_{12} in a much wider temperature and viscosity window, as experiments are generally fast enough so that they do not suffer from degradation problems. The latter method is thus only limited by the fact that one should be able to measure sufficiently accurately zero shear viscosity values, η_0, of each material at each measuring temperature. This is the most important reason why direct measurements of the interfacial tension between PP or POM and pure PPE failed; measurement temperatures to reach break-up in such a case are so high that accurate determination of the zero shear viscosity of the PP or POM phase without polymer degradation becomes impossible.

Other advantages and limitations of each method have been outlined in detail previously in the respective theoretical sections of each method.

5. Conclusions

The influence of the PPE content in a miscible PS/PPE phase on the surface tension and polarity of PS/PPE mixtures, and on the interfacial tension in PP/(PS/PPE) and POM/(PS/PPE) systems has been investigated. Surface tensions, $\sigma(T)$, were experimentally determined by means of the PDA technique, and were compared to values predicted theoretically via Macleod's theory. The interfacial tension, σ_{12}, was determined both from the dynamic breaking thread method and from the PDA, which is an equilibrium method. The results were compared to values predicted from the harmonic mean equation [30]. A good agreement was found between the absolute values for σ_{12} from both the techniques.

The *surface tension* of PS/PPE mixtures in a temperature range of 230–260°C seemed to remain unaffected by the presence of PPE, within the experimental error of the measurements. These findings were in good agreement with the prediction of $\sigma(T)$ from Macleod's theory.

Also the *interfacial tension* of PP/(PS/PPE) or POM/(PS/PPE) systems did not seem to be affected when using a PS/PPE phase with a higher content of PPE. Values of 5.2 ± 0.6 mN/m for the interfacial tension in PP/PS systems and of 9.7 ± 0.7 mN/m in POM/PS systems were measured. These values agree well with the data reported in literature. Comparison of these experimental data from both the techniques, with the predicted interfacial tension via the harmonic mean equation yielded an excellent agreement. Theoretical predictions were shown to be very useful for a better understanding of the influence of the PPE content in the PS/PPE phase because the high melt-viscosity of PS/PPE mixtures containing more than 25% of PPE restricted the applicability of both techniques to a small part of the composition range of the PS/PPE mixtures. It can be seen that higher contents of PPE only lead to minor changes of the interfacial tension, which are however not linearly proportional to the PPE content. The changes are rather small with respect to the experimental error on the measurements, and for mixtures containing only up to 25% PPE are certainly negligible. Finally, calculations showed that PPE causes the polarity of the PS/PPE mixtures to slightly increase from a value of 0.17 for pure PS to 0.20 for pure PPE.

Acknowledgements

Prof Favis is greatly acknowledged for giving us (V.E.) the possibility to perform the breaking thread experiments in his laboratory at the Ecole Polytechnique de Montréal (Quebec, Canada), and Dr Hua Liang for her daily assistance. Juergen Pionteck is indebted for the pendant drop analysis experiments. The authors (V.E. and G.G.) are indebted to the Dow Benelux N.V. Company for the financial support of this project. The FWO (Fund for Scientific Research Flanders) is acknowledged for the financial support of the research stay (V.E.) in Canada in order to perform the breaking thread experiments. FWO and KULeuven Research Council are acknowledged for their financial support in equipment. Dr. ir. Inge Vinckier (KULeuven, Department of Chemical Engineering) is acknowledged for his support in the rheometry experiments. General Electric Plastics (Bergen-op-Zoom, The Netherlands) is aknowledged for supplying the PPE-800. DSM Research (Geleen, The Netherlands) is thanked for giving the possibility of melt-blending the PS/PPE mixtures.

References

[1] Plochocki AP, Dagli SS, Andrews RD. Polym Engng Sci 1990;30:741.
[2] Wu S. Polym Engng Sci 1987;27:335.
[3] Mekhilef N, Favis BD, Carreau PJ. J Polym Sci, Polym Phys 1997;35:293.
[4] Lepers JC, Favis BD. J Polym Sci, Polym Phys 1997;35:2271.
[5] Liang H, Favis BD. Ind Engng Chem Res 1997;36:1211.
[6] Hietaoja PT, Holsti-Miettinen RM, Seppälä JV, Ikkala OT. J Appl Polym Sci 1994;54:1613.
[7] Favis BD, Chalifoux JP. Polym Engng Sci 1987;27:1591.
[8] Favis BD, Chalifoux JP. Polymer 1988;29:1761.
[9] Favis BD, Therrien D. Polymer 1991;32:1474.
[10] Wallheinke K, Pötschke P, Fritsche H, Stutz H. J Appl Polym Sci 1997;65:2217.
[11] Anastasiadis SH, Gancarz I, Kolberstein JT. Macromolecules 1988;21:2980.
[12] Helfand E, Bhattacharjee SM, Frederickson GH. J Chem Phys 1989;91:7200.
[13] Kie HN, Won HJ. Polymer 1995;36:3727.
[14] Ellingson PC, Strand DA, Cohen A, Sammler RL, Carrière CJ. Macromolecules 1994;27:1643.
[15] Broseta D, Frederickson GH, Helfand E, Leibler L. Macromolecules 1990;23:132.
[16] Everaert V, Groeninckx G, Aerts L. Polymer, 2000;41:1011.
[17] Everaert V, Groeninckx G. Book of extended abstracts. In: European Symposium on Polymer Blends, Maastricht, The Netherlands, 12–15 May 1996, vol. 111, 1996.
[18] Schultz AR, Gendron BM. J Appl Polym Sci 1972;16:461.
[19] Prest WM, Porter RS. J Polym Sci, Polym Phys 1972;10:1639.
[20] Aerts L, Dow Benelux NV. Private communication.
[21] Tomotika S. Proc Roy Soc 1935;A150:322.
[22] Tomotika S. Proc Roy Soc 1936;A153:302.
[23] Lord Rayleigh. Proc Roy Soc 1879;29:71.
[24] Chappelear DC. Polym Prepr 1964;5:363.
[25] Palierne JF, Lequeux F. J Non-Newtonian Fluid Mech 1991;40:289.
[26] Luciani A, Champagne MF, Utracki LA. Polym Networks Blends 1996;6:51.
[27] Machiels AGC, Van Dam J, Posthuma de Boer A, Norder B. Polym Engng Sci 1997;37:1512.
[28] Elmendorp JJ. A study on polymer blending microrheology. PhD thesis, Delft University of Technology, 1986.
[29] Kuhn W. Kolloid Z 1953;132:84.
[30] Wu S. Polymer interface and adhesion. New York: Marcel Dekker, 1982.
[31] Elemans PHM, Janssen JMH, Meijer HEH. J Rheol 1990;34:1311.
[32] Cross MM. J Colloid Interface Sci 1970;33:30.
[33] Vinckier I. KULeuven, private communication.
[34] Escudie E, Graciaa A, Lachaise J. Mater Chem Phys 1986;14:239.
[35] Anastasiadis SH, Chen JK, Kolberstein JT, Siegel AF, Sohn JE, Emerson JA. J Colloid Interface Sci 1987;119:55.
[36] Pionteck J, Pötscke P, Uzman M. Book of abstracts. Paper presented at REGIO SURFACE, Freiburg, Germany, 20–22 February 1995, p. 79.
[37] Song B, Springer J. J Colloid Interface Sci 1997;184:64.
[38] Harland S, Hartley RW. Axisymmetric fluid–liquid interfaces. Amsterdam: Elsevier, 1987.
[39] Rotenberg Y, Boruvka L, Neumann AW. J Colloid Interface Sci 1983;93:169.
[40] Springer J, Song B. Pendant drop analysis software. Institute of Technical Engineering, Macromolecular Chemistry, Technische Universität Berlin, Germany, 1992.
[41] Oda Y, Hata T. Preprints, 17th Annual Meeting High Polymer Society, Japan, 1968, p. 267.
[42] Nemirovski N, Siegmann A, Narkis M. J Macromol Sci Phys Ed 1995;B34:459.
[43] Demarquette NR, Kamal MR. Polym Engng Sci 1994;34:1823.
[44] Kamal MR, Lai-Fook R, Demarquette NR. Polym Engng Sci 1994;34:1834.
[45] Pionteck J, Kressler J. Book of extended abstracts. Poster presented at the European Symposium on Polymer Blends, Maastricht, The Netherlands, 12–15 May.
[46] Van Krevelen DW. Properties of polymers. Correlations with chemical structure. Amsterdam: Elsevier, 1992.
[47] Crevecoeur G. PhD thesis, Catholic University of Leuven, Belgium, 1991.
[48] Schoolenberg GE. Shell International Chemicals, Amsterdam, The Netherlands, private communication, 1997.
[49] Brandrup J, Immergut EH, editors. Polymer handbook. New York: Wiley, 1989.
[50] Pham HT, Carriere CJ. Polym Engng Sci 1997;37:636.